diffusion-fundamentals

The Open-Access Journal for the Basic Principles of Diffusion Theory, Experiment and Application

The Technological Impact of Diffusion in Nanopores

Douglas M. Ruthven
Department of Chemical Engineering
University of Maine,
Orono, ME, 04469-5737, USA

ABSTRACT

The impact of nanopore diffusion on the performance of adsorption separation processes is reviewed. Zeolite membrane processes and kinetically selective cyclic adsorption processes depend for their selectivity on differences in intracrystalline diffusion rates so these processes are designed to operate under conditions of intracrystalline diffusion control. In contrast, the performance of equilibrium based adsorption separation processes is adversely affected by diffusional resistance so in such processes the minimization of all resistances to mass transfer is a major design objective. Zeolite catalyzed reactions constitute a further important class of processes in which intrusion of diffusional resistance can be either advantageous or disadvantageous. Such effects are illustrated by considering in detail the conversion of methanol to light olefins (MTO) over SAPO34.

Within the chemical process industries diffusion is important over a wide range of length scales. In this paper we focus only on diffusion at the nanometer scale since diffusional phenomena on this scale are critically important in adsorption separation processes as well as in many heterogeneous catalytic systems. Indeed membrane separations and molecular sieving adsorption processes (kinetic separations) are driven by differences in nanoscale diffusivities. For such processes the conditions of operation must therefore be selected so as to maximize the influence of nanoscale diffusion. This is true also for certain catalytic processes in which product selectivity can sometimes be improved by operating under conditions of diffusion control. More commonly, in equilibrium controlled adsorptive separations and in catalytic systems where activity rather than selectivity is the important feature, process performance is adversely affected by nanoscale diffusion, and in such systems it is obviously desirable to design the process in such a way as to minimize the intrusion of diffusional resistances. Some examples of both classes of process are discussed below.

1. Zeolite Membranes

The possibility of producing thin coherent defect free zeolite membranes that will allow industrially important molecular sieving separations to be carried out as a continuous flow process has attracted much attention over the past decade[1,2]. The removal of water from organics by pervaporation through a type A zeolite membrane is now commercial [3-5]. For several other important separations, including xylenes separation and CO_2 removal from natural gas, promising performance of a zeolite membrane has been demonstrated at laboratory or pilot plant scale and the main barriers to commercialization are associated with problems of scale-up [6-8].

Permeance and Selectivity

The simplest model for a zeolite membrane is similar in concept to the well known solution-diffusion model for a polymeric membrane and assumes a diffusive flux driven by the concentration gradient, in accordance with Fick's first law:

$$J = -D\frac{\partial q}{\partial z} \tag{1}$$

The concentration gradient is provided by the pressure difference across the membrane so, if the equilibrium isotherm is linear ($q^* = Kp$):

$$J = -K\frac{dp}{dz} = \frac{KD}{\ell}\left(p_H - p_L\right) \tag{2}$$

The constant of proportionality between the flux and the pressure difference (KD/ℓ) is commonly referred to as the permeance while the product of the permeance and the membrane thickness (KD) is referred to as the permeability . At low sorbate concentrations (in the linear region of the isotherm) all components of a mixture diffuse independently so the selectivity is given by:

$$S_{AB} = \frac{J_A}{J_B} = \frac{K_A D_A}{K_B D_B} \tag{3}$$

Since the temperature dependences of D and K follow respectively Arrhenius and vant Hoff expressions [$D = D_\infty e^{-E/RT}$; $K = K_\infty e^{-\Delta U/RT}$] the permeance is expected to vary exponentially with reciprocal temperature, either increasing or decreasing depending on the relative magnitudes of E and ΔU. Such behavior is commonly observed at low loadings (see figure 1a)[9]. However at higher loadings the permeance generally passes through a maximum as shown in figure 1b [10]. To understand this behavior it is necessary to recall that the true driving force for diffusive transport is the gradient of chemical potential, rather than the concentration gradient:

$$J = -Bq\frac{\partial \mu}{\partial z} \tag{4}$$

Assuming an ideal Langmuir isotherm with an ideal vapor phase:

$$\frac{q}{q_s} = \frac{bp}{1+bp} \tag{5}$$

The flux is then given by:

$$J = \frac{D_0 q_s}{\ell}\ell n\left[\frac{1+bp_H}{1+bp_L}\right] \tag{6}$$

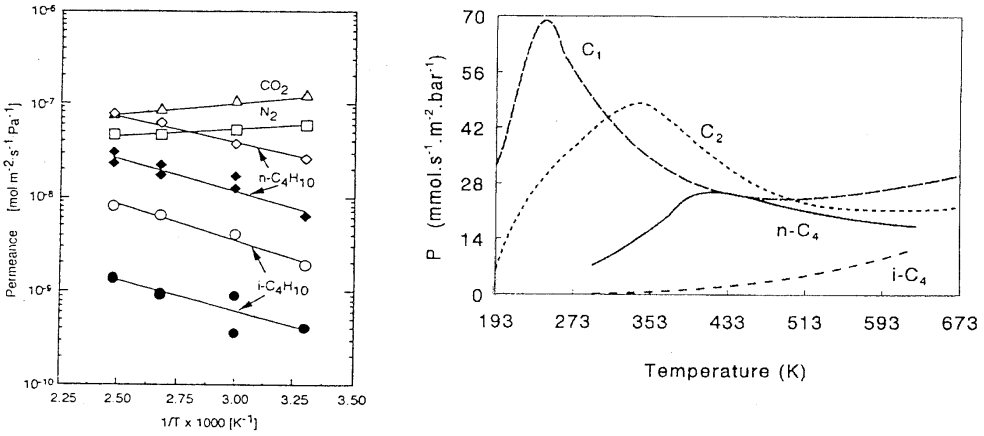

Fig. 1 Temperature dependence of (a) Permeance and (b) Flux for permeation of permanent gases and light hydrocarbons through silicalite membranes.

(a) shows permeance data for N_2, CO_2 and nC_4/iC_4 as a function of reciprocal temperature from data of Kusabe et al.[9] Note that the data for permeation of nC_4 / iC_4 mixtures (filled symbols) show a reduced flux but a higher selectivity suggesting that the permeance of iC_4 is reduced more than that of nC_4 by competitive adsorption.

(b) shows fluxes of CH_4, C_2H_6, C_3H_8 and n/iC_4 plotted as a function of temperature for fixed P_H and P_L taken from data of Bakker et al. [10]

in place of Eq. 2, where D_0 is the thermodynamically corrected transport diffusivity defined by:

$$D_0 \equiv BRT = D\left(\frac{d\ell nq*}{d\ell np}\right) \tag{7}$$

Eq. 6 correctly predicts that, for given values of the upstream and downstream partial pressures (p_H and p_L) the flux [and therefore the permeance defined as $J/(p_H\text{-}p_L)$] will pass through a maximum with temperature, as commonly observed. Note that at low loadings ($bp << 1.0$) Eq. 6 reduces to Eq. 2.

Permselective Separations

In extreme cases where one of the components is sterically excluded from the pore system a highly efficient molecular sieve separation may be achieved (provided that the membrane is coherent). However, large separation factors are achieved only when the larger molecule is completely excluded. If the larger molecule is small enough to enter the pores, albeit slowly, the perm-selectively drops dramatically since in that situation the conditions

for single file diffusion are approached in which all molecules travel at the rate of the slowest. This is illustrated in Table 1 [2].

Table I Separation pattern of an $AlPO_4$-5-in-nickel-membrane foil at 91°C and 1 bar pressure difference over the membrane. Feed: binary mixtures 1:1 of *n*-heptane and an aromatic compound. (From Caro et al[2]).

	n-heptane (single component)	*n*-heptane/ toluene	*n*-heptane/ mesitylen	*n*-heptane/ triethylbenzene	*n*-heptane/ triisopropylbenzene
Flux x 10^6/mole s^{-1} cm^2	3.9	0.85	0.43	1.82	0.94
Flux relative to pure *n*-heptane	100%	22%	11%	47%	24%
Selectivity	-	0.8	1.7	105	1220

Interference effects become important only at relatively high loadings so, when there is a large difference in diffusivity between components, one observes a strong decrease in both flux and selectivity with loading, as illustrated in figure 2 [11].

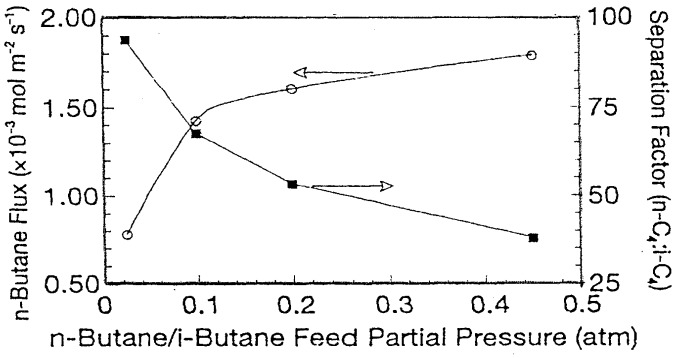

Fig. 2 Variation of flux and selectivity with loading for permeation of nC_4 / iC_4 through a silicate membrane. From Tsapatsis et al. [11]

The perm-selectivity for a mixture is generally found to be lower than the ratio of the pure component permeances (Eq. 3). However, this is not always true. If the faster diffusing species is also the more strongly adsorbed species then, under conditions of competitive adsorption, the adsorption of the slower (and weaker) component will be suppressed by competitive adsorption leading to an *increase* in perm-selectivity [12]. Such an

effect has been observed for n-hexane/dimethyl butane in a silicalite membrane for which separation factors in the mixture are greater than 1,000 in favor of n-hexane [12, 13]. This effect is particularly strong for mixtures containing a fast diffusing but weakly adsorbed species (such as H_2) and a more strongly adsorbed but slower diffusing species [e.g. H_2/SF_6 or CH_4/C_4H_{10}] [14, 15].

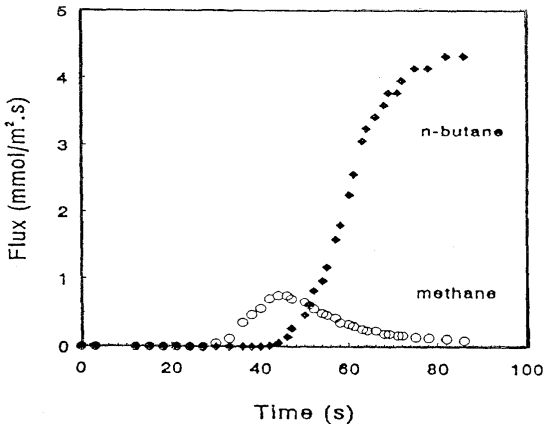

Fig. 3 Transient permeation behavior of a 50-50 binary mixture of CH_4/nC_4H_{10} in a silicalite membrane at 298K. From Geus et al. [16]

At high sorbate loadings the effect of differences in adsorption equilibrium tends to become dominant. Thus for methane/n-butane on a silicalite membrane the pure component diffusivity ratio, at ambient temperature, is about three in favor of methane. However, in the binary mixture the selectivity is inverted leading to preferential permeation of n-butane ($S_{CH4/nC4} \approx 0.06$) [16]. The transient behavior of this system is shown in Figure 3. When a clean silicalite membrane is exposed to a 50-50 binary mixture of methane + n-butane the permeate is initially almost pure methane. The butane penetrates the membrane more slowly so that butane appears in the permeate only after about 45 secs. As the butane flux increases the methane flux declines because the strongly adsorbed butane hinders access of the methane to the pores. If the temperature is increased above 200°C the butane loading decreases to a sufficiently low level that methane again becomes the preferentially permeating species.

Modeling of Permeation in Binary Systems

To properly account for such effects a more sophisticated model is necessary. The most promising approach, developed by Krishna and his associates, is based on the generalized Maxwell-Stefan (GMS) model [17-23]. The basic expression for the flux in a multicomponent system is:

$$\frac{q_i}{RT}\nabla\mu_i = \sum_{s=i}^{n}\frac{q_j N_i - q_i N_j}{q_s Đ_{ij}} + \frac{N_i}{q_s D_{oi}} \tag{8}$$

where D_{oi} represents the thermodynamically corrected transport diffusivity for component i (defined in accordance with Eq. 7) and Đ$_{ij}$ represents the mutual diffusion co-efficient. For a binary Langmuirian system Eq. 8 reduces to:

$$N_A = \frac{-q_s D_{OA}}{1-\theta_A-\theta_B}.\frac{\left(1-\theta_B+\theta_A D_{OB}/Đ_{AB}\right)\frac{d\theta_A}{dz}+\left[\theta_A+\theta_A D_{OB}/Đ_{AB}\right]\frac{d\theta_B}{dz}}{1+\theta_A D_{OB}/Đ_{AB}+\theta_B D_{OA}/Đ_{AB}} \qquad (9)$$

with a similar expression for N_B. When interference between the diffusing species is negligible ($Đ_{AB}\rightarrow\infty$) this reduces to the simplified expression originally derived by Newton, Round and Habgood [24].

The corrected diffusivities (D_{OA}, D_{OB}) can be derived from single component measurements but the mutual diffusivity ($Đ_{AB}$) is not amenable to direct measurement. Krishna has suggested using the Vignes correlation [25] as an estimation method:

$$Đ_{AB} = D_{OA}^{\frac{\theta_A}{\theta_A+\theta_B}}.D_{OB}^{\frac{\theta_B}{\theta_A+\theta_B}} \qquad (10)$$

or, for molecules of different sizes the modified form [26]:

$$q_S Đ_{AB} = \left(q_{SB} D_{OA}\right)^{\frac{\theta_A}{\theta_A+\theta_B}}\left(q_{sOA} D_{OB}\right)^{\frac{\theta_B}{\theta_A+\theta_B}} \qquad (11)$$

where q_{SA} and q_{SB} represent the saturation capacities for the two components.

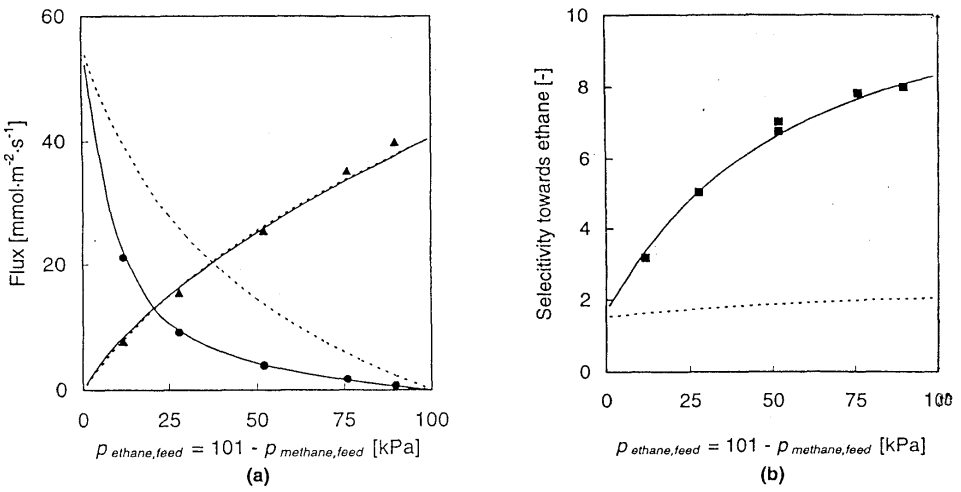

Fig. 4 Separation of C_2H_6/CH_4 mixtures by permeation through a silicalite membrane (a) Flux; (b) Selectivity. Continuous lines show the predictions of the Maxwell-Stefan model (Eq. 9) based on single component values of D_0 with $Đ_{AB}$ estimated from Eq. 11 Dotted lines show predictions of the Habgood model in which mutual diffusion is ignored ($Đ_{AB}\rightarrow\infty$). From van de Graaf *et al.* [21]

This development is based on the ideal Langmuir model for adsorption equilibrium. However the theory can be adapted to incorporate any thermodynamically consistent model for the equilibrium isotherm. The development based on the more realistic ideal adsorbed solution theory (IAS) has been presented by Kapteijn *et al* [22].

Representative comparisons between the experimental permeance and selectivity (for CH_4/C_2H_6-silicalite) and the predictions of the GMS model based on single component data are shown in Figure 4 [25]. Also shown are the corresponding predictions from the Habgood model in which mutual diffusion effects are ignored. For the slower diffusing species (C_2H_6) the predicted flux is only marginally altered by mutual diffusion but for the faster diffusing species (CH_4) the effect of mutual diffusion is considerable so that selectivity predictions based on the simplified Habgood model are substantially in error.

A detailed analysis of the influence of mutual diffusion has been carried out by Karimi and Farooq [27]. They show that the effect is generally small at low loadings but becomes important at high loadings when the difference in the mobilities of the two components is large.

2. **Cyclic Adsorption Separation Processes** (Equilibrium Selectivity)

Because it is difficult to produce a thin coherent zeolite membrane most adsorption separation processes operate in the cyclic mode, under transient conditions, with periodic regeneration by either temperature swing or pressure swing. The majority of such processes depend on differences in adsorption equilibrium to achieve the separation. Such processes operate close to equilibrium so that the more strongly adsorbed species is preferentially adsorbed. The performance of such processes is adversely impacted by intracrystalline (and intraparticle) diffusional resistance so it is a major design objective to minimize these effects.

The simplest example is the selective removal of an undesirable trace impurity (such as H_2S, CO_2 or mercaptans) from a process stream. The practical importance of such processes has increased dramatically in recent years because of the requirement for ultra high purity reagents in the semi-conductor industry. The gas (or liquid) stream to be purified is passed through an adsorption column packed with an adsorbent which has a high equilibrium selectivity (and preferably also a high capacity) for the impurity. Provided that the column is properly designed and operated the impurity can be removed with high efficiency until the column eventually approaches saturation and the impurity starts to "break through" in the effluent. The size of the column and therefore the cost for a given duty depends on the breakthrough capacity which in turn depends on both the equilibrium capacity and the resistance to mass transfer.

To illustrate the importance of diffusional resistance in such a system we consider a trace system with plug flow and a linear isotherm in which the mass transfer rate is approximated by a linear rate expression $\left[d\overline{q}/dt = k\left(q^* - \overline{q}\right)\right]$ with $k=15D/R^2$ – the well known Glueckauf approximation [28]. The breakthrough curves for such a system are given approximately by [29]:

$$\frac{c}{c_O} = \frac{1}{2} erfc\left\{\sqrt{\xi} - \sqrt{\tau} - \frac{1}{8\sqrt{\xi}} - \frac{1}{8\sqrt{\tau}}\right\} \qquad (12)$$

where $\xi = \frac{15D}{R^2}\left(\frac{Kz}{v}\right)\left(\frac{1-\varepsilon}{\varepsilon}\right)$ - dimensionless column length parameter

$\tau = \frac{15D}{R^2}\left(t - z/v\right)$ - dimensionless time parameter

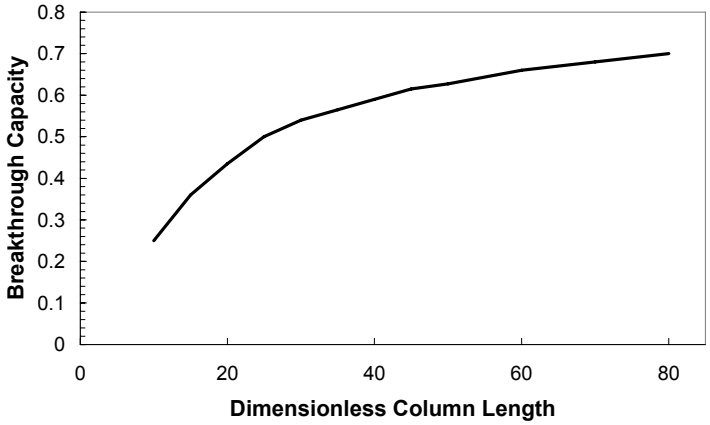

Fig. 5 Variation of dynamic capacity (2% breakthrough) with dimensionless column length parameter for a linear trace system with plug flow and diffusion control.

The ratio ξ/τ represents the hold-up in the column. Assuming an allowable limit for the breakthrough concentration (say c/c_o = 2%) Eq. 12 may be solved to determine the corresponding locus of ξ vs τ and hence the dynamic capacity ξ/τ as a function of column length (ξ). Such a plot is shown in Figure 5. Clearly the reduction in capacity resulting from mass transfer resistance is substantial, and only for a very long column does the dynamic capacity approach the equilibrium capacity.

The dynamic capacity depends on the diffusional time constant (R^2/D) so the performance can clearly be improved by reducing the particle size but only at the cost of an increased pressure drop.

3. Kinetic Separations

There are a number of cyclic adsorption separation processes in which the selectivity depends on differences in adsorption rate rather than on differences in equilibrium. Three representative examples of such processes are given below.

Olefin/Paraffin Separations

The separation of light olefins (C_2 H_4 and C_3H_6) from the corresponding paraffins (C_2H_6 and C_3H_8) has traditionally been carried out by cryogenic distillation [30]. However the difference in boiling points is small so the process is energy intensive and therefore costly. The possibility of developing a more competitive adsorption separation process has therefore attracted much research. The earliest such processes took advantage of the fact that, on cationic zeolites, olefins are adsorbed more strongly than the corresponding paraffins [31]. However, the equilibrium selectivity is relatively modest (K_A/K_B ~ 10) and not sufficiently high to achieve a high purity olefin product at high recovery. The possibility of developing an efficient kinetic separation has therefore attracted much recent attention [32-34].

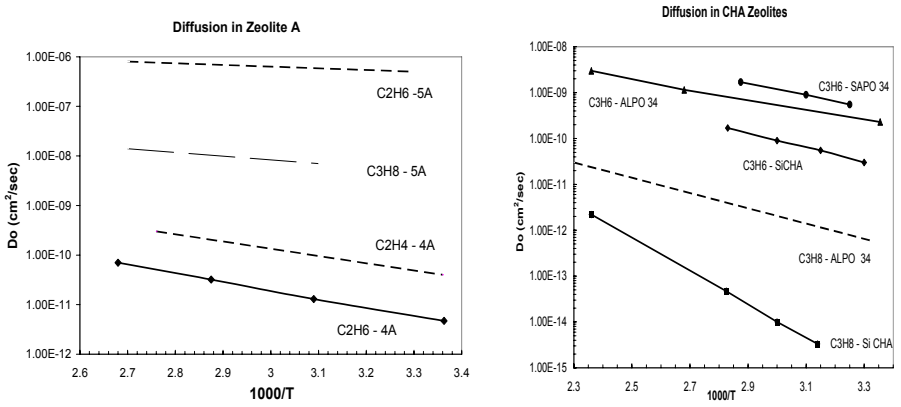

Fig. 6 Arrhenius plot showing the temperature dependence of intracrystalline diffusivity for C_2 and C_3 hydrocarbons in 8-ring zeolites (a) 4A and 5A, (b) various CHA zeolites. Data are from refs 35-38 (a) and 32-34 (b). ZLC data for C_3H_6 - SAPO34 have not been previously reported.

Figure 6 shows diffusivity data for the C_2 and C_3 olefins and paraffins in several different 8-ring zeolites. In 5A zeolite diffusion of the C_2 species is not significantly constrained by steric hindrance so the diffusional activation energy is low (~ 1.5 kcal/mole) with little difference in diffusivity between C_2H_4 and C_2H_6. Steric hindrance is substantially greater in 4A zeolite resulting in higher diffusional activation energies and significantly faster diffusion of C_2H_4, which is the slightly smaller molecule. However, in zeolites of the CHA family, the pores of which are controlled by distorted 8-rings, the differences in diffusivity between olefins and paraffins are much greater (3 to 4 orders of magnitude for C_3H_6/C_3H_8 on high Si CHA). Comparative uptake curves for this system are shown in Figure 7.

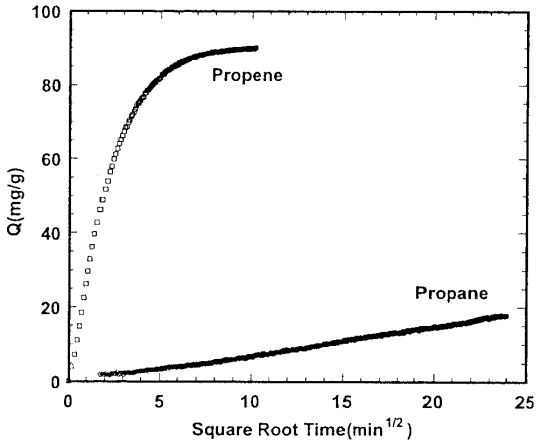

Fig. 7 Comparative (integral) uptake curves for C_3 H_6 and C_3H_8 in SiCHA at 80º C, 600 Torr. From Olson et al.[33] Note that the curves show linearity in $\sqrt{t}$ in the initial region as expected for diffusion control.

The window dimensions and hence the diffusivity and the diffusivity ratio are correlated with the unit cell size (see Figure 8). Si CHA, which has the smallest cell size, has the highest kinetic selectivity but the diffusion of propylene is rather slow, thus restricting the cycle time. The choice between a high selectivity with slow uptake of propylene and a lower selectivity with faster uptake thus represents an interesting optimization problem.

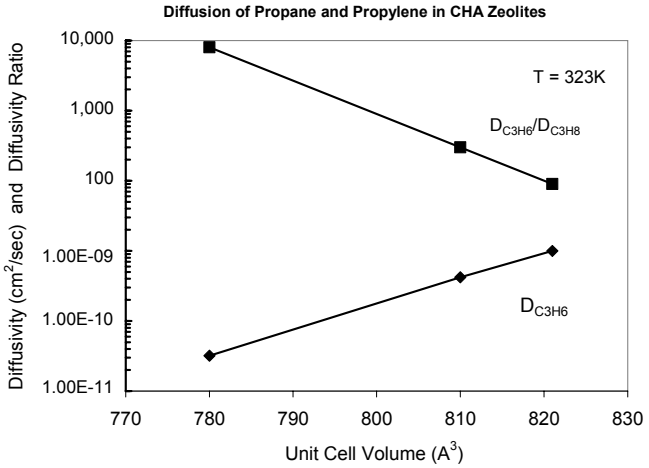

Fig. 8 Variation of diffusivity and diffusivity ratio with unit cell size, for diffusion of C_3H_6 and C_3H_8 in various CHA zeolites.

Air Separation on Carbon Molecular Sieves

Carbon molecular sieves (CMS) adsorbents are produced by pyrolysis of carbonaceous materials followed by carefully controlled deposition of carbon within the pores [39]. In contrast to activated carbons which have a broad distribution of micropore size (generally in the 10 – 100 Å range) the pores of a carbon molecular sieve are very small (< 10 Å) and the pore size distribution in narrow. As a result the adsorption behavior is similar to that of a zeolite.

Carbon molecular sieves are widely used for production of nitrogen from air (by selective adsorption of oxygen). There is little difference between the equilibrium isotherms of O_2 and N_2 on CMS but as a result of its slightly smaller molecular size oxygen is adsorbed very much faster (diffusivity ratio 10 – 100). The sorption kinetics show some interesting features.

Detailed studies show that the sorption kinetics are controlled by a combination of surface resistance and internal diffusion although, depending on the particular adsorbent and the conditions, one or other of these resistances may be dominant [40-43]. The uptake curves (Figure 9) show a clear transition from surface barrier control in the initial region to diffusion control at long times. The differential diffusivity and the surface mass transfer coefficient both increase strongly with loading; much more strongly than is predicted by the thermodynamic correction factor (Eq. 7). The data are correlated by the empirical expressions:

$$\frac{D}{D_0} = 1 + \beta \frac{\theta}{1-\theta}; \quad \frac{k}{k_0} = 1 + \beta^1 \frac{\theta}{1-\theta} \tag{13}$$

where for N_2 $\beta = \beta^1 = 1.8$ and for O_2 $\beta = 0.76$, $\beta^1 = 0.89$. Note that for $\beta = 0$ these expressions reduce to the Darken correction for a Langmuir isotherm since $d\ell nq/d\ell np = 1-\theta$ (see Eq. 7).

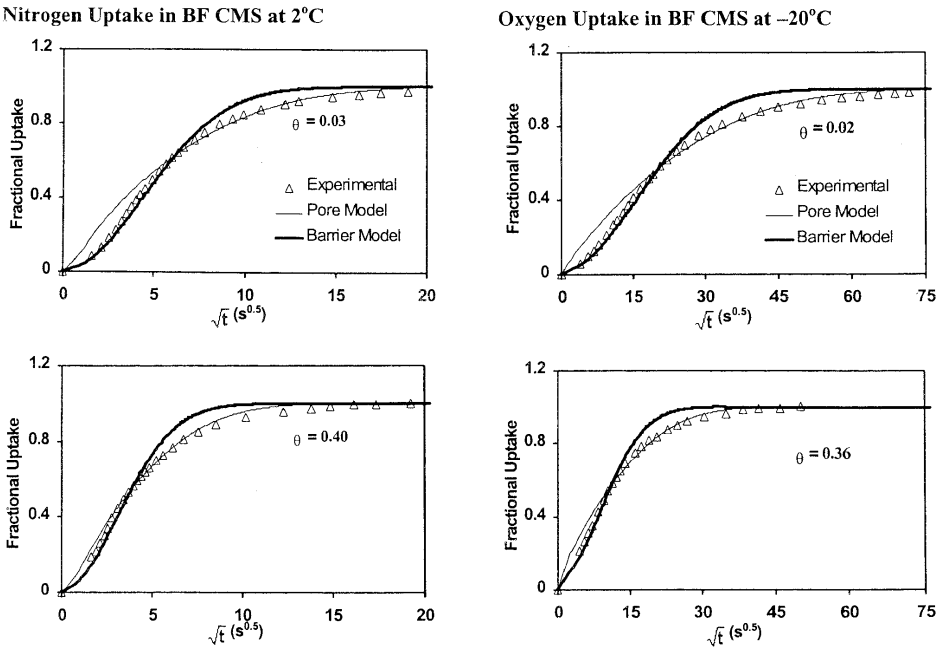

Fig. 9 Representative uptake curves for N_2 and O_2 in Bergbau-Forschung CMS at 298K and various loading levels (θ) showing transition from surface barrier control in the initial region to diffusion control in the long time region. From Sundaram *et al.*[42].

Ding *et al* [44] have recently shown that this behavior can be explained by the pore size distribution of the CMS adsorbents if it is assumed that the diffusional activation energy varies with pore size according to a gamma function distribution.

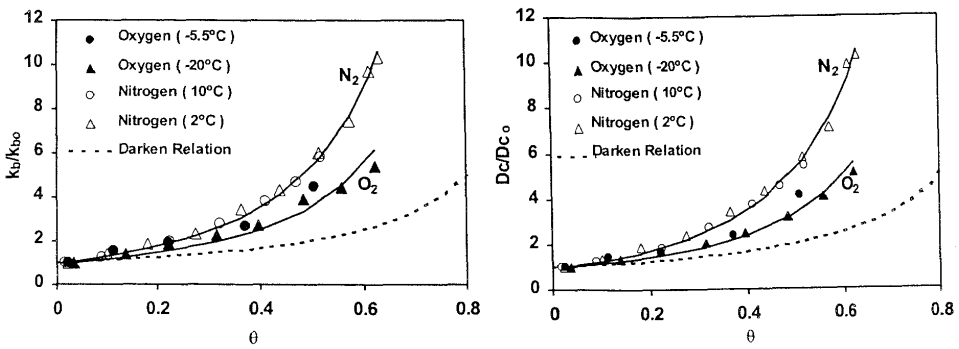

Fig. 10 Variation of (a) surface mass transfer coefficient and (b) internal diffusivity with loading for O_2 and N_2 in BF CMS at 298K. From Sundaram et al.[42]

N_2/CH_4 Separation over ETS-4

Titanosilicalites such as ETS-4 represent a new class of crystalline microporous molecular sieves, similar to zeolites in their general structure but significantly different in their composition. Like the small pore zeolites ETS-4 has a three dimensional channel structure controlled by 8-membered oxygen rings but the dimensions of the unit cell and hence both the size and shape of the 8-ring windows change dramatically with the dehydration temperature [45]. Provided that the thermal stability limit (~ 200°C for Na form, 330°C for Sr form) is not exceeded this effect is reversible. This flexibility endows these adsorbents with a unique "tuneability" that allows the dimensions of the molecular sieve to be optimized to achieve a particular separation (see Fig. 11). So far the most important industrial application of these materials is in the purification of nitrogen rich natural gas (CH_4).

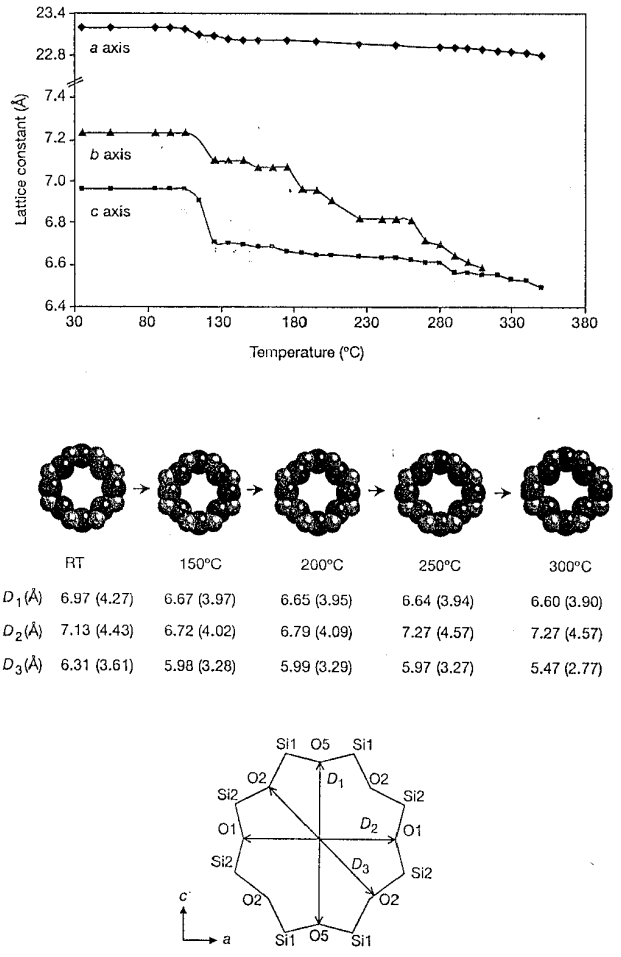

Fig. 11 Variation of lattice parameters and pore dimensions of ETS-4(Sr) with dehydration temperature. Modified from Kuznicki *et al.* [45]

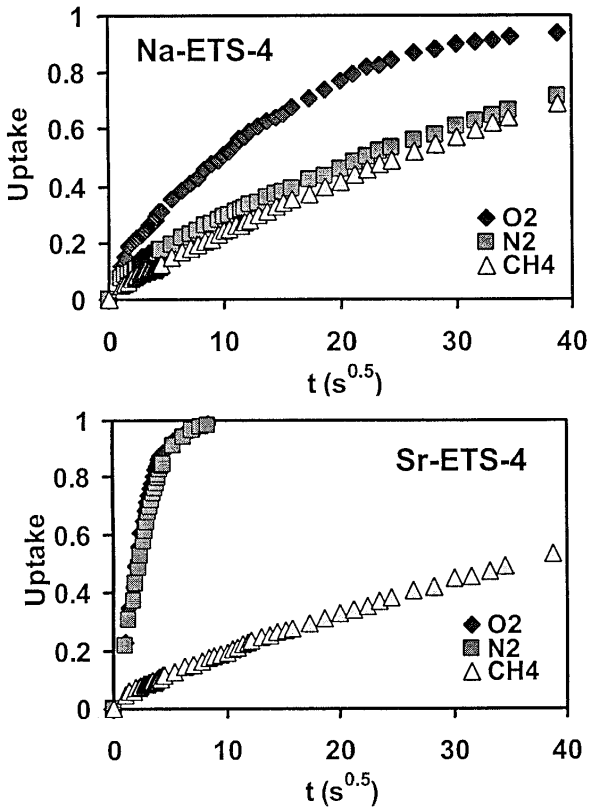

Fig. 12 Uptake curves for O_2, N_2 and CH_4 in SrETS-4 (dehydrated at 270ºC). Data from Farooq *et al.*[46]

To meet the calorific value specification for pipeline grade gas the nitrogen content must not exceed about 4%. Many deposits of natural gas, however, contain much larger concentrations of nitrogen. Cryogenic distillation is uneconomic and on both zeolite and CMS adsorbents N_2 and CH_4 are similarly adsorbed with respect to both equilibrium and kinetics, so the search for an economically viable process for nitrogen removal presented the gas industry with an important challenge. The use of ETS-4 dehydrated at 270°C, appears to be a promising solution since this material shows a high kinetic selectivity for N_2 over CH_4 (see Figure 12), thus allowing an effective kinetic separation to be achieved [46]. Following successful pilot plant trials a full scale unit has been developed using a relatively fast cycle (time scale of minutes) pressure swing adsorption process. About 75% of the N_2 is removed with 95% recovery of CH_4. However, the process is not without its problems:

1. The capacity of the adsorbent is relatively low so a large volume of adsorbent is needed.
2. It is essential to dry the feed gas to very low humidity levels.
3. Methane diffuses into the structure albeit slowly, necessitating periodic thermal regeneration of the adsorber beds. This adds significantly to the process cost.

4. Catalytic Reactions

Diffusion plays a major role in influencing both the activity and selectivity of many catalysts. For a first order reaction in a spherical catalyst particle the intrinsic rate constant (k) is reduced by a factor η (the effectiveness factor):

$$k_e = k\eta$$
$$\eta = \frac{3}{\Phi}\left[1 - \frac{1}{Tanh\Phi}\right] \qquad (14)$$
$$\Phi = R\sqrt{k/D}$$

This basic analysis is commonly attributed to Thiele (1938) [48] and the dimensionless parameter Φ is commonly called the Thiele modulus although essentially the same analysis was published many years earlier by Jüttner [49].

In a zeolite catalyst diffusional limitations may occur at either the particle scale or the crystal scale. In the latter case the basic analysis remains the same but since the rate constant is defined with respect to the concentration of reactant in the vapor phase while the intracrystalline diffusivity is defined with respect to the adsorbed phase concentration, the Thiele modules must be re-defined to introduce the dimensionless adsorption equilibrium constant (K):

$$\Phi_s = R\sqrt{k/KD} = \left(\frac{R^2}{D}.\frac{k}{K}\right)^{1/2} \qquad (15)$$

Both the intrinsic rate constant and the effective diffusivity (KD) can be extracted from measurements of the reaction rate with different size fractions of the zeolite crystals. This approach has been demonstrated by Haag [50] for cracking of n-hexane on HZSM5 and by Post *et al* [51] for isomerization of 2,2 dimethyl butane over HZSM-5.

The methanol to olefins (MTO) reaction offers a more modern example of a catalytic reaction controlled by intracrystalline diffusion. Stimulated by the escalating demand for light olefins, this reaction has attracted much recent attention. The reaction of methanol at 350-450^{o}C over HZSM5 yields a wide spectrum of products including light alkanes, light olefins and single ring aromatics [52-54]. The yield of $C_2^=$ + $C_3^=$ (the desirable product for polyolefin feedstock) amounts to only 30 – 40 %. The introduction of SPO-34 (a structural analog of chabazite) as the catalyst [55] gave a dramatic improvement in both selectivity and conversion, making the process much more attractive. Under properly selected conditions light olefin yields ($C_2^=$ + $C_3^=$) approaching 80% can be achieved with only small amounts of higher olefins and paraffins and essentially no aromatics [56].

The absence of aromatic products appears to be related to the size of the CHA cage which is too small to allow the formation of a benzene ring. The reaction mechanism has been established in broad outline [57, 58] although many important details are still not fully understood:

1. $2CH_3OH \rightarrow CH_3.O.CH_3 + H_2O$
2. $CH_3.O.CH_3 \rightarrow C_2H_4 + H_2O$ (16)
3. $1.5\ C_2H_4 \rightarrow C_3H_6$

Slow polymerization to higher molecular weight species (coke) also occurs. Reaction 3 is reversible and exothermic; this probably accounts for the observed increase in $C_2^= + C_3^=$ yield with temperature.

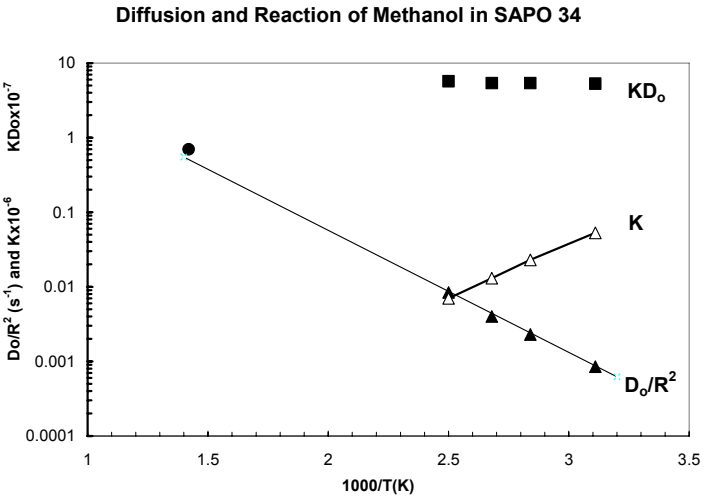

Fig 13 Variation of diffusional time constant (D_0/R^2), dimensionless Henry constant (K) and the product KD_0 with temperature. (From data of Chen *et al* [59]). The value of D_0/R^2 derived from the reaction rate measurements (●) is also shown. Corrected diffusivities are derived from the reported integral diffusivities according to the analysis of Garg and Ruthven [66]

Detailed studies of the kinetics of this reaction over different size fractions of SAPO-34 crystals together with measurements of the sorption rate and the equilibrium isotherm have been reported by Chen *et al* [59-63]. These data are summarized in figure 13. The dominance of intracrystalline diffusion in controlling the sorption rate was shown by varying the crystal size. Values of the diffusional time constant (R^2/D_o) derived from reaction rate measurements at 698K are close to the value extrapolated from sorption rate measurements at lower temperatures with the same batch of SAPO-34 crystals [59,60]. The temperature dependence of the dimensionless Henry constant, also shown in figure 13, yields an adsorption energy of $\Delta U \approx$ -7.5 kcal/mole which is almost the same as the diffusional activation energy derived from the temperature dependence of the (corrected) diffusivity (E = 7.3 kcal/mole.) Consequently the product KD_0, referred to by Chen as the "steady state diffusivity" is almost independent of temperature. A similar situation was noted by Garcia and Weisz [64, 65] in their study of the reaction of various aromatics over HZSM-5.

As the catalyst ages, the light olefin yield and the selectivity both increase [59, 61]. This appears to be related to the build up of coke within the intracrystalline pores which reduces both the intrinsic rate constant and the intracrystalline diffusivity [60, 61]. Detailed

measurements with different crystal sizes show that with increasing coke levels the diffusivity declines more rapidly than the rate constant so that diffusional limitations become more pronounced as the catalyst ages. A high yield of light olefins requires that the DME formed in the first step of the reaction be retained within the crystal long enough for it to be essentially fully converted by reaction 2. This requires that the ratio of the Thiele module should be large:

$$\frac{\Phi_2}{\Phi_1} = \left(\frac{k_2}{k_1} \frac{D_{MeCH}}{D_{DME}} \right)^{\frac{1}{2}} >> 1$$

The *ratio* of the Thiele moduli is independent of crystal size, so in accordance with experimental observations [56], varying the crystal size has no effect on the yield.

Since $k_2 < k_1$ a high ratio of D_{MeOH}/D_{DME} is necessary to achieve a high ratio Φ_2/Φ_1 and thus a high olefin yield. As the DME molecule is larger than the methanol molecule it is reasonable to assume that, under sterically restricted conditions, the diffusivity ratio D_{MEOH}/D_{DME} will increase as the effective pore size decreases. The observations that the olefin yield increases as the catalyst cokes and that an improvement in yield is obtained by increasing the Si/Al ratio (which decreases the unit cell size and therefore the effective window size) are consistent with this hypothesis. However varying the Si/Al ratio also changes the strength of the acid sites so such evidence is not entirely conclusive.

5. Concluding Remarks

The influence of nanopore diffusion on catalytic processes and adsorptive separations is ubiquitous. In most situations these effects are deleterious, leading to reduced reaction rates, reduced selectivity and decreased separation factors. However, molecular sieve membrane processes, kinetic separations and certain catalytic processes depend on differences in micropore diffusivities between different components and, for such systems, process conditions must be selected to maximize the influence of nanopore diffusion. There are numerous examples of such systems in the process industries; those discussed here provide only a brief overview to illustrate the general considerations involved in the design and optimization of these types of system.

Notation

b	Langmuir equilibrium constant (atm^{-1})	q	adsorbed phase concentration
B	mobility	q_s	saturation limit
c	gas phase concentration of sorbate	R	particle radius or gas constant
D	diffusivity	S_{AB}	selectivity
D_0	thermodynamically corrected diffusivity (see Eq. 7)	T	absolute temperature
		v	interstitial gas velocity
$Đ_{AB}$	mutual diffusivity	z	distance coordinate
J	flux	Φ	Thiele modulus
k	reaction rate constant	θ	fractional saturation (q/q_s)
K	Henry's Law constant	β, β^1	constants in Eq. 13
ℓ	membrane thickness	ξ, τ	defined in Eq. 12
p	partial pressure		

References

1. J. Stöcker ed. *Microporous and Mesoporous Mats.* **38**, 1-115 (2000). Special Issue: "Microporous and Mesoporous Membranes and Membrane Systems"

2. J. Caro, M. Noack, P. Kölsch and R. Schäfer *Microporous and Mesoporous Mats.* **38**, 3-24 (2000)

3. H. Kita Int. Workshop on Zeolite Membranes and Fiches – Post Conference of ICIM-5 Gifu, Japan (1998). Proceedings p. 43-46 Japan Assoc. of Zeolites and Membrane Soc. of Japan.

4. H. Kita, K. Horii, Y. Otoshi, K. Tanaka and K. Okamota *J. Mat. Sci. Letters* **14**, 206 (1995) and also in Proc. 7th Int. Conf. on Pervaporation Processes, p. 364 R. Bakish ed. Bakish Mats, Englewood (1995).

5. J. Caro Membranes: "On the Interplay of Diffusion and Permeation and the Technical Consequences" *Adsorption* - in press.

6. NGK Inc. "p-Xylene Production Costs Lowered by new Zeolite Membrane" in *Japan Chemical Week*, Nov. 7th (2002)

7. J.H. Hedlund, J. Sterte, M. Athonis, A.-J .Bons, B. Carstensen, E.W. Corcoran, D.M. Cox, H.W. Deckman, W. De Gijnst, P.-P. de Moor, F. Lai, J. McHenry, W. Mortier, J.J. Reinoso and J. Peters "High Flux MFI Membranes" *Microporous and Mesoporous Materials* **52**,179-189 (2002)

8. T. Tomita, K. Nakayama and H. Satari *Microporous and Mesoporous Mats.* **68**, 71-75 (2004)

9. K. Kusabe, A. Murata, T. Kuroda and S. Morooka *J. Chem. Eng. Japan* **30**, 72-78 (1997)

10. W.J.W. Bakker, F. Kapteijn, J. Poppe and J.A. Moulijn *J. Membrane Sci.* **117**, 57-78 (1996)

11. M. Tsapatsis and G.R. Garda *MRS Bulletin* **1**, 30 (1999)

12. J. Falconer *Int. Workshop on Zeolite Membranes* Post Conf. ICIM 98, Gifu, Japan, Proceedings p. 21 (1998)

13. J. Coronas, R.D. Noble and J.L. Falconer *Ind. Eng. Chem. Res.* **37**, 166 (1998)

14. R.D. Noble and J.L. Falconer *Catalysis Today* **25**, 209 (1995)

15. Z.A.E.P. Vroom, K. Keizer, M.J. Gilder, H. Verweij and A.J. Burgraaf *J. Membrane Sci.* **113**, 293 (1996)

16. E.R. Geus, H. Van Bekkum, W.J.W. Bakker and J.A. Moulijn *Micoroporous Mats.* **1**, 131 (1993)

17. R. Krishna and J.A. Wesselingh *Chem. Eng. Sci.* **52**, 861-911 (1997)

18. F.J. Keil, R. Krishna and M.O. Coppens *Rev. Chem. Engg* **16**, 71-197 (2000)

19. R. Krishna and R. Baur *Sep. and Purif. Technol.*, 1-42 (2003)

20. R. Krishna and L.J.P. van den Broecke *Chem. Eng. J.* **57**, 155 (1995)

21. J.M. van de Graaf, F. Kapteijn and J.A. Moulijn *A.I.Ch.E. Jl* **45**, 497-511 (1999)

22. F. Kapteijn, J.A. Moulijn and R. Krishna *Chem. Eng. Sci*. **55**, 2923-2930 (2000)

23. R. Krishna and R. Baur *Chem. Eng. J.* **97**, 37-54 (2004)

24. G.F. Round, H.W. Habgood and R. Newton *Sep. Sci.* **1**, 219 (1996)

25. A. Vignes, *Ind. Eng. Chem. Fund.* **5**, 189-199 (1966)

26. A.I. Skoulidas, D.S. Sholl and R. Krishna *Langmuir*, (2003 or 2004)

27. I.A. Karimi and S. Farooq *Chem. Eng. Sci.* **55**, 3529-3541 (2000)

28. E. Glueckauf *Trans. Faraday Soc.* **51**, 1540 (1955)

29. D.M. Ruthven *Principles of Adsorption and Adsorption Processes* p. 236 John Wiley, New York (1984)

30. R. B. Eldridge *Ind. Eng. Chem. Res.* **32**, 2208-2212 (1993)

31. D.L. Peterson, F. Helfferich and R.K. Griep in *Molecular Sieves*. Proc. 1st Int. Zeolite Conf. London 1967 p. 217-229. Published by Soc. Chem. Ind., London (1968)

32. D. Olson U.S. Patent 6,488,741 B2 Dec. 3 2002

33. D. Olson, M.A. Camblor, L.A. Villaescusa and G.H. Kühl *Microporous and Mesoporous Materials*, **67,** 27-33 (2004)

34. S.C Reyes *et al* U.S. Patent 6,730,142 B2 May 4 2004

35. Z. Xu, M. Eic and D.M. Ruthven Ninth Int. Zeolite Conf., Montreal 1992. *Proceedings*, vol. 2 p. 147R. von Ballmoos, J.B. Higgins and M.M.J. Travers eds. Butterworth, Stoneham, MA, (1993)

36. J. Kärger and D.M. Ruthven *J.Chem.Soc. Faraday Trans. I*, **77,** 1485 (1981)

37. H. Yucel and D.M. Ruthven *J.Chem.Soc. Faraday Trans. I*, **76**, 60-70 (1980)

38. A.C. Sheth, M.Sc. Thesis, Northwestern University, Evanston IL (1969)

39. H. Jüntgen, K. Knoblauch and K. Harder, *Fuel*, **60**, 817 (1981). See also *Adsorption Sci. and Technol.* **158**, 269-283. A.E. Rodigues *et al* eds. Kluwer, Dordrecht (1988)

40. K.F. Loughlin, M.M. Hassan, A.I. Fatehi and M. Zakur, *Gas Sep. Purif.* **7**, 264-273

41. D. Shen, M. Bülow and N. Lemcoff *Adsorption* **9** 295-302 (2003)

42. S.M. Sundaram, H. Qinglin and S. Farooq 7th Int. Conf. on Fundamentals of Adsorption, Nagasaki, May 2001. *Proceedings.*

43. S. Farooq and S.K Bahtia – personal communication

44. L.P. Ding, Y.X. Yuan, S. Farooq and S.K. Bahtia *Langmuir* – in press

45. S.M. Kuznicki, V.A. Bell**,** S. Nair, H.W. Hillhouse, R.M. Jacubinas, C-M. Braunbath, B.H. Toby and M. Tsapatsis *Nature* **412**, 720-724 (2001)

46. R.P. Marathe, K. Mantri, M.P. Srinivasan and S. Farooq "Effect of Ion Exchange and dehydration temperataure on Adsorption and Diffusion of Gases in ETS-4"

47. M. Mitariten. *American Oil and Gas Reporter* p. 103-104 Mar. 2001

48. E.W. Thiele *Ind.Eng.Chem.* **31**, 916 (1939)

49. F. Jüttner *Z. Phys.Chem.* **65,** 595 (1909)

50. W.O. Haag, R.M. Logo and P.B. Weisz *Disc. Faraday Soc.* **72**, 317 (1982)

51. M.F.M. Post, J. van Amstel and H.W. Kouwenhoven p. 517 in Proc. 6th Int. Zeolite Conf. Reno, Nevada, 1983. D. Mason and A. Bisio eds. Butterworth, Guildford, UK (1984)

52. C.D. Chang, C.T.W.Chu and R.F. Socha *J. Catal* **86**, 289 (1984)

53. N.Y. Chen, W.E. Garwood and F.G. Dwyer *Shape Selective Catalysis in Industrial Operations* p. 233-238. Marcel Dekker, New York (1989)

54. C.D. Chang in *Methanol Production and Use*, Chapter 4 p. 133-173, Marcel Dekker New York.

55. S.W. Kaiser. U.S.Patent 4,499,327 (1985)

56. S. Wilson and P. Barger *Microporous and Mesoporous Materials* **29,** 117-126 (1999)

57. G.F. Froment, W.J.H. Dehertog and A.J. Marchi Ch. I *Catalysis* Vol. 9 J.J. Spivey ed. Royal Soc. Chemistry, London (1992)

58. I.M. Dahl and S. Kolkoe *J. Catalysis* **149,** 458-464 (1994) and **161,** 304-309 (1996)

59. D. Chen, H.P. Rebo, K. Moljord and A. Holman *Ind.Eng.Chem.Res.* **38**, 4241-4249 (1999)

60. D. Chen, H.P. Rebo, and A. Holman *Chem.Eng.Sci.* **54,** 3465-3473 (1999)

61. D. Chen, H.P. Rebo, K. Moljord and A. Holman *Ind.Eng.Chem.Res.* **36,** 3473-3479 (1997)

62. D. Chen, H.P. Rebo, K. Moljord and A. Holman *Chem.Eng.Sci.* **51,** 2687-2692 (1996)

63. D. Chen, H.P. Rebo, K. Moljord and A. Holman *Studies Surf.Sci.Catalysis* **119,** 521 (1998)

64. S.F. Garcia and P.B. Weisz *J.Catalysis* **121,** 294-311 (1990)

65. S.F. Garcia and P.B. Weisz *J.Catalysis* **142**, 691-696 (1993)

66. D.R. Garg and D.M. Ruthven *Chem.Eng.Sci.* **27,** 417 (1972)

APPENDIX

Fundamentals of Adsorption Equilibrium and Kinetics in Nanoporous Adsorbents

Adsorption Equilibrium

The simplest model for adsorption equilibrium is the ideal Langmuir isotherm:

$$\frac{q^*}{q_s} = \frac{bp}{1+bp}$$

If bp << 1 this reduces to Henry's Law:

$$q^* = (bq_s)p$$

with bq_s equal to the Henry constant. For analysis of adsorption kinetics it is useful to express the Henry constant in dimensionless form:

$$K = (\partial q^*/\partial c)_{T=} \rho RTbq_s$$

where q_s is expressed in moles/gm and ρ is the density of the adsorbent.

Adsorption Kinetics

If the rate of sorption is controlled by surface resistance the uptake curve, for a set of uniform spherical particles of radius *R* subjected to a step change in ambient concentration at t=0 is given by:

$$\frac{m_t}{m_\infty} = 1 - \exp\left[-\frac{3kt}{R}\right]$$

or in the initial region $m_t/m_\infty \approx 3kt/R$.

The corresponding expression for internal diffusion control is:

$$\frac{m_t}{m_\infty} = 1 - \frac{6}{\pi^2}\sum_{n=1}^{\infty}\frac{1}{n^2}\exp\left[-n^2\pi Dt / R^2\right]$$

or, equivalently:

$$\frac{m_t}{m_\infty} = 6\left(\frac{Dt}{R^2}\right)^{\frac{1}{2}}\left[\frac{1}{\sqrt{\pi}} + 2\sum_{n=1}^{\infty} ierfc\left(\frac{nR}{\sqrt{Dt}}\right)\right] - \frac{3Dt}{R^2}$$

For short times this reduces to:

$$\frac{m_t}{m_\infty} = \frac{6}{\sqrt{\pi}}\sqrt{\frac{Dt}{R^2}}$$

The short time behavior (proportionality with either t or $\sqrt{t}$) thus provides evidence concerning the nature of the controlling resistance (surface barrier or internal diffusion) and a simple way to estimate the time constant ($R/3k$ or R^2/D).

Chemical Potential Gradient as Driving Force

The relationship between the Fickian diffusivity (D) and the thermodynamically corrected diffusivity (D_0) based on chemical potential gradient as the driving force is: [29]

$$D = D_0\left(\frac{\partial \ln p}{\partial \ln q*}\right)_T$$

For a Langmuir isotherm this reduces to:

$$D = \frac{D_0}{1-\theta}$$

where $\theta = q/q_s$.

Although in principle both D and D_0 are dependent on loading it turns out that, for many systems the variation of D_0 is quite modest so, as a first approximation, one can often assume that D_0 is a function only of temperature.